Electrophotonic enhancement of bulk heterojunction organic solar cells through photonic crystal photoactive layer

John R. Tumbleston,[1,a)] Doo-Hyun Ko,[2] Edward T. Samulski,[2] and Rene Lopez[1]
[1]*Department of Physics and Astronomy, University of North Carolina, Chapel Hill, North Carolina 27599, USA*
[2]*Department of Chemistry, University of North Carolina, Chapel Hill, North Carolina 27599, USA*

(Received 18 July 2008; accepted 24 December 2008; published online 27 January 2009)

We present one- (1D) and two-dimensional (2D) periodic nanostructured designs for organic photovoltaics where a photonic crystal is formed between blended poly-3-hexylthiophene/[6,6]-phenyl-C61-butyric acid methyl ester (P3HT:PCBM) and nanocrystalline zinc oxide. Absorption enhancements over the full absorption range of P3HT:PCBM of 20% (one polarization) and 14% are shown for the 1D and 2D structures, respectively. These improvements result in part from band edge excitation of quasiguided modes. The geometries are also shown to create excitons 26% (1D) and 11% (2D) closer to P3HT:PCBM exit interfaces indicating further photovoltaic improvement. © *2009 American Institute of Physics*. [DOI: 10.1063/1.3075053]

Inexpensive, organic, semiconducting photovoltaic (PV) materials have been actively explored since Tang[1] reported 1% efficiency energy conversion in an organic solar cell in 1986. Currently, attention is focused on bulk heterojunction devices[2] wherein the organic donor-acceptor pair is phase separated on a scale of tens of nanometers to facilitate the splitting of the exciton, a bound electron-hole pair, into free carriers. Along with the bound exciton, organic PV materials have an intrinsic drawback relative to inorganic semiconductors: poor electron-hole transport.[3] Furthermore, PV conversion is especially low near the band edge due to weak absorption. Hence, a geometry that could simultaneously enhance band edge absorption and electronic transport would be very advantageous in this class of PV materials.

In this letter, we posit designs for one- (1D) and two-dimensional (2D) periodic nanostructured photonic crystal (PC) photoactive layers that could boost performance through enhanced optical absorption and a beneficial redistribution of exciton formation. We demonstrate our design with a popular organic PV material, the bulk heterojunction blend of poly-3-hexylthiophene (P3HT) and [6,6]-phenyl-C61-butyric acid methyl ester (PCBM), but our rationale could be applied to other organic and inorganic PV materials. Our design features a broad enhancement over the full spectral range of P3HT:PCBM with substantial increases closer to the band edge where the extinction coefficient is smallest.

Light trapping schemes (diffraction gratings,[4] optical spacer layers,[5] and folded substrates[6]) have been explored in organic PV devices where improvements were noted. Cell designs that incorporate well-ordered PCs have also shown promise for inorganics[7,8] because specifically desired regions of the solar spectrum can be targeted for enhancement. This was explored in theoretical[9] and experimental[10] studies of a PC composed of an ordered heterojunction of an electron donating polymer and PCBM, but the currently accessible length scale of the PC (hundreds of nanometers) is not commensurate with the length scale for exciton migration (tens of nanometers[11]). Furthermore, photonic properties depend greatly on the index of refraction contrast between the two PC materials,[12] and there is a relatively small contrast between the electron donor, P3HT, and PCBM.[9] Herein, we propose a PC photoactive layer consisting of the P3HT:PCBM bulk heterojunction blend and a porous form of nanocrystalline zinc oxide (nc-ZnO) with an index of refraction around 1.4. We further show that this geometry is able to create excitons closer to the P3HT:PCBM exit interfaces. After exciton harvesting in the P3HT:PCBM, free carriers may be more suited to readily escape from the photoactive blend resulting in enhanced electrical performance.

Consider the nanostructured PC device designs shown in Fig. 1. Both *p*- and *s*-polarized light are incident on the relatively thick glass substrate where reflection from the air-glass interface is disregarded. Light then enters the stack/PC and may be trapped as a quasiguided mode.[13] The latter is a

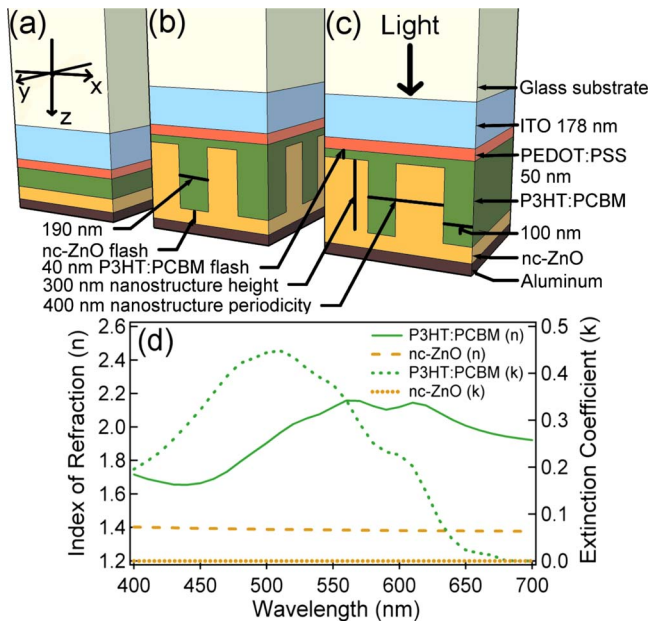

FIG. 1. (Color online) Illustration of three organic PV device designs: (a) conventional planar PV stack (control device), (b) square posts with 395 nm 2D square periodicity, and (c) channels with 400 nm 1D periodicity. (d) Optical properties of the two PC materials, P3HT:PCBM and nc-ZnO.

[a)]Electronic mail: tumblest@physics.unc.edu.

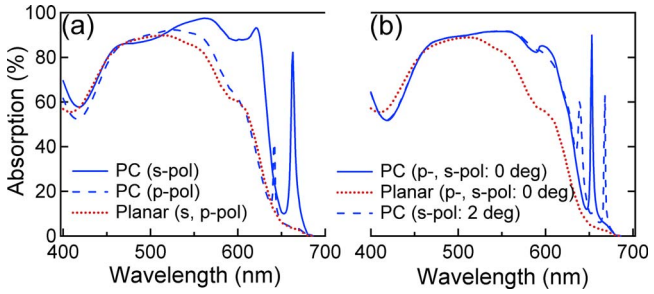

FIG. 2. (Color online) (a) Theoretical spectral absorption at normal incidence for 400 nm 1D periodic PC device compared to planar control cell for both *s*- and *p*-polarized light. (b) Spectral absorption for 395 nm 2D periodic posts at both normal incidence (both polarizations) and 2° incidence (*s*-polarization only).

partially trapped or leaky mode excited in the photoactive region leading to sharp enhancements in absorption as shown near the band edge of Fig. 2. Excitation of these modes is solely a consequence of the PC topography of the PV layer with high index of refraction contrast. Furthermore, there are enhancements across the whole spectrum ($\lambda = 400-685$ nm) for both the 1D and 2D periodic device designs that result in integrated 20% (*s*-polarization) and 14% (both polarizations) enhancements, respectively. Multiplying the absorption by the AM 1.5 solar spectrum[14] in this spectral range and integrating causes essentially no change in the enhancement factors.

Exploiting the light management offered by a PC, the height and periodicity are chosen to provide enhancements near the band edge of P3HT:PCBM. The polarization also has a strong dependence as shown in Fig. 2(a) for the 1D periodic device where there is only a 2% integrated spectral increase for incident light that is *p*-polarized (electric field perpendicular to the periodicity in the *x*-direction) compared to 20% enhancement for *s*-polarization. Furthermore, the incident angle plays a role in quasiguided mode excitation as shown in Fig. 2(b) where *s*-polarized absorption is calculated at 2° incidence. It is clear that mode excitation is dependent on the incident parameters and device optical and physical properties. As a rough estimate, the spectral location of quasiguided modes can be determined using an empty lattice approximation for the photonic band structure.[13]

The absorption models presented above and the local exciton creation profiles presented later were computed using the scattering matrix formulism.[13] The complex dielectric functions of each cell material in Fig. 1 are used as input in the model and were measured using spectroscopic ellipsometry. The optical parameters for the two PC materials, P3HT:PCBM and nc-ZnO, are given in Fig. 1(d). The measured optical properties agree closely with literature [P3HT:PCBM;[15] glass, indium tin oxide (ITO), poly(3,4-ethylenedioxythiophene):poly(styrenesulfonate) (PEDOT:PSS);[16] aluminum (Al)[17]]. The porous form of nc-ZnO was synthesized following Ref. 18. The glass substrate, ITO, PEDOT:PSS, and nc-ZnO are taken to be transparent over the entire spectral range, so the presented absorption only includes optical losses in the blend that lead to exciton formation. The Al back reflector/electrode is a slightly lossy material, so even greater absorption could be realized using an optimized back reflector, such as a PC stack.[7]

In order to make true comparisons between PC and planar control designs, we require each to have equivalent volumes of P3HT:PCBM blend. The 1D and 2D periodic designs were tailored to improve performance over control devices with blend thicknesses of ~110 nm, which is the approximate thickness previously studied for planar devices with an optical spacer.[5] The effect of interference on absorption is also important when defining the control device. We account for interference effects by increasing the nc-ZnO flash layer thickness (the pure nc-ZnO layer below the nanostructured layer) and the nc-ZnO film thickness for the control device up to 500 nm while integrating the spectral absorption at each step. We only compare absorption spectra that show maximum integrated absorption for both the PC and control devices.

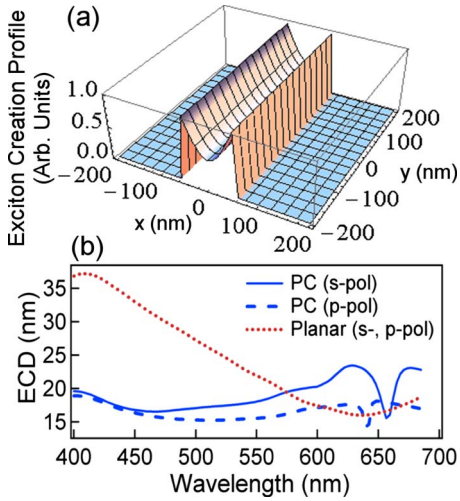

FIG. 3. (Color online) (a) Exciton creation profile of one unit cell for the 1D periodic device at a depth of 150 nm with an incident *p*-polarized wavelength of 550 nm at normal incidence. (b) Spectral ECD for the 1D periodic device and planar control at normal incidence.

Along with the absorption enhancements previously shown (Fig. 2), we also show that excitons are created closer to nanostructured P3HT:PCBM exit interfaces (with either the PEDOT:PSS or nc-ZnO) than in a planar device. The exciton creation profile is the final step in an optics model before electronic processes such as exciton splitting and free carrier transport occur.[19] Calculating the proximity of exciton creation to exit interfaces provides a rough estimate of potential electronic transport enhancements in the PC device even though no electronic processes are considered. In general, the exciton creation profile is given by the time-averaged monochromatic pointwise energy dissipation per unit time per unit area $\langle Q \rangle$,

$$\langle Q \rangle = \frac{\pi c \epsilon_0 \epsilon_2 |\vec{E}|^2}{\lambda}, \tag{1}$$

where ϵ_2 is the imaginary part of the spatially dependent dielectric function, ϵ_0 is the permittivity of vacuum, c is the speed of light in vacuum, λ is the free space wavelength, and $|\vec{E}|$ is the magnitude of the spatially dependent complex electric field. For the photoactive layer in conventional planar device stacks, both $|\vec{E}|$ and $\langle Q \rangle$ are adequately taken to be only functions of depth z, while ϵ_2 is a constant.[19] The exciton creation profile for one unit cell for the 1D periodic PC device for $\lambda = 550$ nm at a depth of $z = 150$ nm into the 300 nm nanostructured layer is given in Fig. 3(a) to show how local absorption varies over the lateral directions, x and y.

There is no absorption around each channel because they are surrounded by transparent nc-ZnO. By weighting the profile against the shortest distance l, to a P3HT:PCBM blend exit interface with either the PEDOT:PSS or nc-ZnO, the exciton creation distance (ECD) for a given incident wavelength, angle, and polarization can be determined,

$$\mathrm{ECD} = \frac{\int_V \langle Q \rangle l d\tau}{\int_V \langle Q \rangle d\tau}, \tag{2}$$

where the integrals are taken over one unit cell of the entire photoactive P3HT:PCBM volume (flash and nanostructure).

ECD values are shown over the entire spectrum for the 1D periodic structure at normal incidence in Fig. 3(b). It is noticed that the greatest reductions occur toward the blue spectral end where absorption is essentially equal between PC and the control devices (Fig. 2). The comparable ECDs become closer near the band edge where absorption is stronger for the PC device. Ultimately, this indicates an overall improved PV performance over the entire spectrum either due to shortened ECDs (blue end) or stronger absorption (red end). The presence of the quasiguided modes is again realized with this calculation where sharp reductions are visible near the band edge. These modes have the effect of concentrating absorption in the thin P3HT:PCBM flash layer, which results in reduced ECD values.

By averaging over the full spectral range, the channel structure yields average ECD reductions of 30% (*p*-polarization) and 22% (*s*-polarization) when compared to the planar device. Likewise, the 2D periodic spectral ECD reduction is 11%. These improvements are promising and full 2D and 3D solutions of the transport equations[20] should be conducted to determine how this geometry affects recombination and the exciton dissociation probability, which also dictate the overall electronic performance.

In conclusion, we demonstrated that a PC comprised of a photoactive layer of P3HT:PCBM bulk heterojunction blend and nc-ZnO can simultaneously enhance optical absorption and produce excitons closer to exit interfaces in P3HT:PCBM. Overall spectral absorption enhancements for the 1D and 2D periodic structures are 20% (one polarization) and 14%, respectively, with larger improvements observed near the band edge. Furthermore, ECDs are reduced by 26% and 11% for the respective PC designs.

Two of the authors, J.T. and R.L., acknowledge support from the Army Research Office Grant No. W911NF-07–1-0539, while D.K. and E.S. were supported by NSF (NIRT: Bio-Inspired Actuating Structures Grant No. CMS-0507151) and NASA (URETI Biologically Inspired Materials Grant No. NAG-1–2301).

[1] C. W. Tang, Appl. Phys. Lett. **48**, 183 (1986).
[2] G. Yu and A. J. Heeger, J. Appl. Phys. **78**, 4510 (1995).
[3] K. M. Coakley and M. D. McGehee, Chem. Mater. **16**, 4533 (2004).
[4] M. Niggemann, M. Glatthaar, A. Gombert, A. Hinsch, and V. Wittwer, Thin Solid Films **451–452**, 619 (2004).
[5] J. Y. Kim, S. H. Kim, H.-H. Lee, K. Lee, W. Ma, X. Gong, and A. J. Heeger, Adv. Mater. (Weinheim, Ger.) **18**, 572 (2006).
[6] S.-B. Rim, S. Zhao, S. R. Scully, M. D. McGehee, and P. Peumans, Appl. Phys. Lett. **91**, 243501 (2007).
[7] L. Zeng, Y. Yi, C. Hong, J. Liu, N. Feng, X. Duan, L. C. Kimerling, and B. A. Alamariu, Appl. Phys. Lett. **89**, 111111 (2006).
[8] P. Bermel, C. Luo, L. Zeng, L. C. Kimerling, and J. D. Joannopoulos, Opt. Express **15**, 16986 (2007).
[9] D. Duche, L. Escoubas, J.-J. Simon, P. Torchio, W. Vervisch, and F. Flory, Appl. Phys. Lett. **92**, 193310 (2008).
[10] M.-S. Kim, J.-S. Kim, J. C. Cho, M. Shtein, L. J. Guo, and J. Kim, Appl. Phys. Lett. **90**, 123113 (2007).
[11] P. W. M. Blom, V. D. Mihailetchi, L. J. A. Koster, and D. E. Markov, Adv. Mater. (Weinheim, Ger.) **19**, 1551 (2007).
[12] J. D. Joannopoulos, R. D. Meade, and J. N. Winn, *Photonic Crystals: Molding the Flow of Light* (Princeton University Press, New Jersey, 1995), p. 41.
[13] S. G. Tikhodeev, A. L. Yablonskii, E. A. Muljarov, N. A. Gippius, and T. Ishihara, Phys. Rev. B **66**, 045102 (2002).
[14] Reference Solar Spectral Irradiance, Air Mass 1.5, http://rredc.nrel.gov/solar/spectra/am1.5/.
[15] F. Monestier, J.-J. Simon, P. Torchio, L. Escoubas, F. Flory, S. Bailly, R. de Bettignies, S. Guillerez, and C. Defranoux, Sol. Energy Mater. Sol. Cells **91**, 405 (2007).
[16] H. Hoppe, N. S. Sariciftci, and D. Meissner, Mol. Cryst. Liq. Cryst. Sci. Technol., Sect. A **385**, 113 (2002).
[17] E. D. Palik, *Handbook of Optical Constants of Solids* (Academic, Orlando, 1985), p. 369.
[18] W. J. E. Beek, M. M. Wienk, M. Kemerink, X. Yang, and R. A. J. Janssen, J. Phys. Chem. B **109**, 9505 (2005).
[19] N.-K. Persson, H. Arwin, and O. Inganas, J. Appl. Phys. **97**, 034503 (2005).
[20] L. J. A. Koster, E. C. P. Smits, V. D. Mihailetchi, and P. W. M. Blom, Phys. Rev. B **72**, 085205 (2005).